Probing Receptor-Translocator Interactions in the Oligopeptide ABC Transporter by Fluorescence Correlation Spectroscopy

Mark K. Doeven,* Geert van den Bogaart,* Victor Krasnikov,† and Bert Poolman*
*Department of Biochemistry and †Ultrafast Laser Spectroscopy Laboratory, Groningen Biomolecular Sciences and Biotechnology Institute and Zernike Institute for Advanced Materials, University of Groningen, 9747 AG Groningen, The Netherlands

ABSTRACT The oligopeptide transporter Opp is a five-component ABC uptake system. The extracytoplasmic lipid-anchored substrate-binding protein (or receptor) OppA delivers peptides to an integral membrane complex OppBCDF (or translocator), where, on ATP binding and hydrolysis, translocation across the membrane takes place. OppA and OppBCDF were labeled with fluorescent probes, reconstituted into giant unilamellar vesicles, and the receptor-translocator interactions were investigated by fluorescence correlation spectroscopy. Lateral mobility of OppA was reduced on incorporation of OppBCDF into giant unilamellar vesicles, and decreased even further on the addition of peptide. Fluorescence cross-correlation measurements revealed that OppBCDF distinguished liganded from unliganded OppA, binding only the former. Addition of ATP or its nonhydrolyzable analog AMP-PNP resulted in release of OppA from OppBCDF. In vanadate-trapped "transition state" conditions, OppA also was not bound by OppBCDF. A model is presented in which ATP-binding to OppDF results in donation of peptide to OppBC and simultaneous release of OppA. ATP-hydrolysis would complete the peptide translocation and reset the transporter for another catalytic cycle. Implications in terms of a general transport mechanism for ABC importers and exporters are discussed.

INTRODUCTION

ABC transporters compose one of the largest protein families, and their function and dysfunction are in a number of cases linked to human diseases (1,2). ABC transporters catalyze the unidirectional transport of a wide variety of substrates over cellular and organellar membranes and are widely distributed throughout all forms of life. Two hydrophobic TMDs create the translocation pathway, and two peripherally associated NBDs fuel the transport reaction by binding and hydrolyzing ATP. Directionality of the translocation process can be deduced from the presence or absence of a fifth component, the extracytoplasmic SBP (also termed receptor). ABC efflux systems lack this constituent, whereas in bacterial ABC importers the SBP is essential for function.

A vast amount of experimental data is available for different ABC efflux systems, and although mechanistic details may differ in individual cases, a consensus model on how this type of transporters work is emerging (3,4). Substrate is bound at a high-affinity cytoplasmic facing binding site, located within the TMDs. ATP-binding induces NBD dimerization and reorientation of the loaded substrate-binding site from a high affinity inside- to a low affinity outside-facing conformation. After substrate release, ATP-hydrolysis resets the transporter by opening the NBDs and reorienting the empty binding site.

Data on SBP-dependent ABC importers are limited to one or two systems as an experimentally well supported transport mechanism is currently available only for the maltose permease $MalEFGK_2$ from *Escherichia coli* (5–7) and, to a lesser extent, the histidine permease $HisJQMP_2$ from *Salmonella typhimurium* (8,9). In a series of elegant experiments, Davidson and colleagues showed that liganded SBP MalE, while bound to the TMDs (MalF and G), opens on ATP-binding to the NDBs (two copies of MalK per functional complex). In the vanadate-trapped transition state for ATP-hydrolysis, MalE, in its open conformation, is bound tightly to $MalFGK_2$, whereas the affinity for maltose is reduced. Under posthydrolysis conditions MalE dissociates from $MalFGK_2$, thereby resetting the transporter for the next catalytic cycle. These data contrast those of the vitamin B_{12} transporter Btu, where SBP BtuF binds tightly to BtuCD in the absence and presence of MgATP, and might not dissociate from the transporter during the catalytic cycle (10). In fact, the recent crystal structure of the BtuCD-F complex reveals BtuF in (at least partial) open conformation (11), suggesting a posttranslocation state of BtuCD with tightly bound, unliganded SBP.

The oligopeptide ABC transporter OppABCDF from *Lactococcus lactis* is composed of an extracytoplasmic lipid-anchored SBP, OppA, two TMDs, OppB and C, and two

Submitted September 2, 2007, and accepted for publication December 21, 2007.

Address reprint requests to Bert Poolman, Dept. of Biochemistry, Groningen Biomolecular Sciences and Biotechnology Institute and Zernike Institute for Advanced Materials, Nijenborgh 4, 9747 AG Groningen, The Netherlands. Tel. 31-50-3634190; Fax. 31-50-3634165; E-Mail: b.poolman@rug.nl.

Mark K. Doeven's present address is Dept. of Pediatrics, Center for Liver, Digestive and Metabolic Diseases, University Medical Center Groningen, Hanzeplein 1, PO Box 30.001, 9700 RB Groningen, The Netherlands.

Abbreviations used: ABC, ATP-binding cassette; DDM. *n*-dodecyl-β-D-maltoside; FCS, fluorescence correlation spectroscopy; FCCS, fluorescence cross-correlation spectroscopy; GUV, giant unilamellar vesicle; LUV, large unilamellar vesicle; NBD, nucleotide-binding domain; SBP, substrate-binding protein; TMD, transmembrane domain.

Editor: Thomas Schmidt.

0006-3495/08/05/3956/10 $2.00

doi: 10.1529/biophysj.107.120964

NBDs, OppD and F, bound to the cytosolic face of the TMDs (12). In vitro transport assays with purified proteins reconstituted in LUVs suggested that OppBCDF specifically recognizes liganded OppA (13). This finding contrasted with observations for the maltose and histidine transporters, where unliganded SBP seemed to have access to the TMDs as well, thereby inhibiting transport activity (14–16).

We now used purified and fluorescent-labeled OppA and OppBCDF, incorporated into giant unilamellar vesicles, to probe the interactions between the receptor and translocator of the oligopeptide ABC transporter, using fluorescence auto- and cross-correlation spectroscopy (17). Based on the results, a model for oligopeptide transport is presented which shows similarities but also differences compared with the mechanism proposed for the maltose permease. The possible origins for the observed differences are discussed, thereby increasing our knowledge on the translocation mechanism of SBP-dependent ABC transporters.

EXPERIMENTAL PROCEDURES

Bacterial strain and growth conditions

C-terminal His_6-tagged OppA, OppA I602C, and OppBCDF (His_6-tag on C-terminus of OppC) were produced in *L. lactis* AMP2/pAMP31, NZ9000/pNZOppA (I602C) and NZ9000/pAMP42, respectively, as described (13,18, 19). C-terminal His_6-tagged LacS C320A/A635C was produced by *E. coli* HB101, using the pSKE8his expression vector as described (19). Plasmid pAMP42 (OppC I296C) was an intermediate product in the construction of pNZOppA (I602C) and was used for production of OppBC(I296C)DF by *L. lactis* NZ9000. Cells were grown in 5% (w/v) whey-permeate, 0.5% (w/v) yeast extract, 0.5% (w/v) glucose, and 65 mM KPi, pH 7.0, supplemented with 5 μg/mL chloramphenicol in volumes of 10 L in a bioreactor with pH control (ADI 1065 fermentor; Applikon Dependable Instruments B. V., Schiedam, The Netherlands). The pH was kept constant at pH 6.5 by titrating with 2 M KOH. Trancription from the *nisin A* promoter (plasmid constructs in strain NZ9000) was induced at an OD_{660} of 2 by adding 1:1000 (v/v) of the culture supernatant of *L. lactis* NZ9700. Cells were harvested by centrifugation, washed with 100 mM KPi, pH 7.0, resuspended in 100 mM KPi, pH 7.0, plus 20% (v/v) glycerol, and stored at −80°C.

Protein purification and fluorescent labeling

OppA and OppBCDF were purified as described (13,18). OppA I605C and LacS C320A/A635C were purified and labeled with Alexa Fluor 488 C5 maleimide (Invitrogen) as described (19). Labeling of OppA I605C and LacS C320A/A635C with Alexa Fluor 633 C5 maleimide (Invitrogen) was done in exactly the same way as previously described for Alexa Fluor 488 C5 maleimide (19). OppBC(I296C)DF was purified and labeled with either Alexa Fluor 488 or Alexa Fluor 633 as follows. Membrane vesicles were prepared by rupturing the cells with a high-pressure homogenizer (Kindler Maschinen AG, Zürich, Switzerland) in the presence of 20% (v/v) glycerol. OppBC(I296C)DF containing membranes were resuspended to 5 mg/mL of total membrane protein in 50 mM KPi, pH 8.0, 200 mM KCl, and 20% (v/v) glycerol (buffer A), and solubilized with 0.5% (w/v) DDM. After 12 min of centrifugation at 280,000 × *g* and 4°C, the supernatant was diluted five times with buffer A and incubated with nickel-nitrilotriacetic acid resin (0.05 mL/mg of total membrane protein) for 1.5 h at 4°C while shaking gently. Subsequently, the resin was poured into a column and washed with 20 column volumes of buffer A, supplemented with 0.05% (w/v) DDM and 10 mM imidazole. Labeling was done by incubating the purified protein while bound to the column for 2 h up to overnight at 4°C with an ~30 times molar excess of probe dissolved in five column volumes buffer A plus 0.05% (w/v) DDM. The column was washed with 20 column volumes buffer A plus 0.05% (w/v) DDM to remove free label, and the labeled OppBC(I296C)DF complex was eluted in the same buffer, pH 7.0, supplemented with 100 mM histidine. The degree of labeling was estimated by measuring the absorbance of Alexa Fluor 488 and 633 (extinction coefficients are 71,000 $M^{-1}cm^{-1}$ at 495 nm and 100,000 $M^{-1}cm^{-1}$ at 633 nm, respectively) and determination of protein concentration and was found to be 80–100% for each protein preparation. The protein concentrations were estimated from A280 measurements (the extinction coefficients of OppA, OppBCDF, and LacS are 1.605, 0.990, and 0.926 $(mg/mL)^{-1}cm^{-1}$, respectively) and corrected for absorption at 280 nm by the Alexa Fluor dyes.

Reconstitution of (fluorescent-labeled) Opp proteins in LUVs and GUVs

Triton X-100 mediated incorporation of the fluorescent-labeled Opp proteins into LUVs was done as described (for specific details see Doeven and colleagues (13); for generic procedure see Poolman and colleagues(20) and Rigaud, Pitard, and Levy (21)). First, OppBC(I296C)DF was reconstituted at a 1:20 or 1:100 (w/w) protein/lipid ratio as specified further in the Results. Second, OppA(I602C) was attached to (OppBC(I296C)DF containing) liposomes at a 1:50 (w/w) protein/lipid ratio, which corresponds to ~3.5 nmol $OppA/m^2$ of membrane surface (13). Third, Opp-containing LUVs were converted into proteo-GUVs, essentially as described (19). Briefly, proteo-LUVs in 50 mM NH_4HCO_3, pH 8.0, were frozen and thawed three times in the presence of 0.1 g of sucrose/g lipids. 10 μL proteo-LUVs (5 mg/mL lipids) were dried on an ultraviolet-ozone cleaned cover-slide under a gentle stream of nitrogen gas, followed by an overnight incubation under vacuum at 4°C. Rehydration was done by adding 500 μL of 20 mM K-Hepes, pH 8.0. GUV formation was monitored by fluorescence microscopy. Optionally, bradykinin (a nonameric peptide with the amino acid sequence RPPGFSPFR) and/or nucleotides were included in the rehydration buffer. The distributions of peptide and/or nucleotide on the inside and outside of the GUVs after vesicle formation was assessed in control experiments by including tracer amounts (~10 nM) of Oregon Green 488-labeled RPPGFSPFC or Alexa Fluor 647-ATP (Invitrogen) in the rehydration buffer, followed by confocal imaging of the formed GUVs (see below). At the concentrations of peptide and nucleotides used, i.e. 20 μM and 0.1 – 3 mM, respectively, no significant differences between the amounts of solutes present inside and outside the proteo-GUVs could be detected.

Activity of fluorescent-labeled Opp

Activity of the fluorescent-labeled proteins was determined as described previously by measuring peptide binding (OppA; (18)) and/or peptide transport (OppABCDF; (13)). These measurements were performed at 30°C.

Confocal imaging, FCS and FCCS measurements

FCS measurements were carried out at 18°C on a dual-color laser scanning confocal microscope. For the measurements, 10 μL proteo-LUVs (5 mg/mL lipids), rehydrated in 500 μL of 20 mM K-Hepes, pH 8.0, w/wo peptide and/or nucleotides (see figure legends) were used. A carefully optimized amount of sucrose was added to the proteo-LUVs before the dehydration step (0.1 g sucrose/g lipids; (19)). Sucrose protects the proteins by providing critical hydrogen bonds on dehydration and suppressing the liquid crystalline-gel phase transition in the membrane on dehydration-rehydration (and thereby prevents the proteins from aggregating) (19). Too much sucrose, albeit not unfavorable for the proteins, inhibited GUV formation. Local variations in the sugar concentration and of the dried lipid layer most likely caused the observed heterogeneities in fluorescence intensity within a single sample of

GUVs. These heterogeneities reflect differences in protein/lipid ratios between the GUVs; the diffusion coefficients of the proteins in the different GUVs are presented in Supplementary Material, Fig. S1. At high protein/lipid ratios the mobility of OppA tended to decrease weakly, as one would expect, because the mean free path of diffusion decreases. However, the observed heterogeneities in protein/lipid ratio of both OppA and OppBCDF did not significantly correlate with the diffusion constant (Spearman's rho, $P = 5\%$; Fig. S1).

The laser scanning confocal microscope is based on an inverted microscope Axiovert S 100 TV (Zeiss, Jena, Germany) in combination with a galvanometer optical scanner (model 6860, Cambridge Technology, Watertown, MA) and a microscope objective nano-focusing device (P-721, PI). The two laser beams (488 nm, argon ion laser, Spectra Physics and 633 nm, He-Ne laser, JDS Uniphase) were focused by a Zeiss C-Apochromat infinity-corrected 1.2 NA 63× water immersion objective for excitation of the Alexa Fluor 488 and 633 fluorophores. The fluorescence was collected through the same objective, separated from the excitation beams by a beam-pick off plate (BSP20-A1, ThorLabs) and split into two channels by a dichroic beam splitter (585dcxr, Chroma Technology, Rockingham, VT), and finally directed through emission filters (HQ 535/50 and HQ675/50, Chroma Technology) and pinholes (diameter of 30 μm) onto two avalanche photodiodes (SPCM-AQR-14, EG&G). The fluorescence signals were digitized and auto- and cross-correlation curves were calculated using a multiple τ algorithm.

The setup was calibrated by measuring the known diffusion coefficients of Alexa Fluor 488 and 633 in water (Invitrogen; $D = 300\ \mu m^2/s$). The lateral radii ω_{xy}, defined as the point were the fluorescence count rate dropped e^2 times, were 180 nm for Alexa fluor 488 and 240 nm for Alexa fluor 633. Overlap of the two confocal volumes for dual-color FCCS experiments was optimized by maximizing the cross-correlation signal of double-labeled DNA, which was made by annealing equimolar amounts of 5′-ATTATTGAGTGGTCACTTTAAA-3′ labeled on the 5′-end with Alexa Fluor 488 and 5′ TTTAAAGTGACCACTCAATAAT-3′ labeled on the 5′-end with Alexa Fluor 633 (IBA, St. Louis, MO). The overall efficiency of the fluorescence cross-correlation was found to be better than 80%. Crosstalk was lower then 5%. Auto- and cross-correlation curves were fitted with a one-component three- (22) or two-dimensional diffusion model (23). Two-component fits were attempted in selected experiments; however, these did not yield interpretable data because of the relatively small changes observed in diffusion coefficients and the large errors between the measurements.

Miscellaneous

Mutations were confirmed by restriction analysis and DNA sequencing. Protein concentrations of membrane vesicles were determined according to a modified version (BioRad DC protein assay) of the method of Lowry et al. (24), using bovine serum albumin as a standard. The concentrations of purified OppA and OppBCDF were determined before reconstitution into LUVs by measuring the absorption at 280 nm and using extinction coefficients of 1.605 and 0.990 $(mg/mL)^{-1}cm^{-1}$, respectively.

RESULTS

Lateral mobility of OppA is reduced in OppBCDF-containing GUVs

Previous experiments showed that the lateral mobility of lipid-anchored OppA in GUVs was comparable to that of fluorescent lipids (19), which is consistent with the Saffman-Delbrück model for Brownian motion in biological membranes (25). Since the mobility of integral membrane proteins was 2–3 times lower than that of OppA (19), we anticipated that we could monitor the binding of OppA to its cognate membrane complex by autocorrelation analysis. Binding of fluorescent-labeled OppA to OppBCDF would result in a reduced mobility of the labeled protein. A single-cysteine mutant of OppA, OppA (I602C), was labeled with Alexa Fluor 488 and reconstituted at a 1:50 (w/w) protein/lipid ratio, which corresponds to ~3.5 nmol OppA/m^2 of membrane surface (13). OppBCDF was coreconstituted at a 1:20 (w/w) protein/lipid ratio, resulting in approximately equal amounts of OppA and OppBCDF complex molecules in the membrane. At these concentrations, according to the estimated K_M of OppBCDF for liganded OppA (~1.75 nmol/m^2; 13), most OppBCDF complexes are interacting with OppA provided the OppAs are in the peptide-bound state. In Table 1 the results of the autocorrelation measurements are presented. In OppBCDF-containing GUVs, the mobility of OppA was lowered compared with vesicles devoid of OppBCDF, which could reflect binding or is because of increased membrane crowding. The dissociation constant (K_D) for binding of bradykinin (peptide with the sequence RPPGFSPFR) to OppA is 0.1 μM (18,26). On addition of 10 μM bradykinin, that is, when all the OppA molecules are in the ligand-bound state, OppA diffusion slowed down from 3.1 ± 0.4 to 2.3 ± 0.5 ($\times\ 10^{-8}$ cm^2/s). In vanadate-trapped transition state conditions, that is, in the presence of substrate, MgATP and *ortho*-vanadate (Vi), OppA mobility was again as fast as without peptide ($3.2 \pm 0.3 \times 10^{-8}$ cm^2/s). In the absence of peptide, however, no distinction could be made between OppA binding to OppBCDF and reduced lipid mobility in general as a consequence of the mere presence of OppBCDF (increased crowding). A similar reduction in mobility compared to fluorescent-labeled OppA was observed for the

TABLE 1 Lateral mobility of OppA in OppBCDF-containing GUVs

Protein composition of GUVs		Additions to rehydration buffer		
OppA-AF488*	OppBCDF†	10 μM bradykinin	3 mM MgATP plus 0.5 mM Vi	Diffusion coefficient (10^{-8} cm^2/s)‡
+	−	−	−	7.5 ± 1.8
+	+	−	−	3.1 ± 0.4
+	+	+	−	2.3 ± 0.5
+	+	+	+	3.2 ± 0.3

*OppA (I602C) labeled with Alexa Fluor 488 was reconstituted at a 1:50 (w/w) protein/lipid ratio.
†OppBCDF was reconstituted at a 1:20 (w/w) protein/lipid ratio.
‡Diffusion coefficients represent the average of at least two independent experiments of at least five measurements each, and the SD values are given. The FCS setup was calibrated with free Alexa probes.

fluorescent lipid analog DiO (from 7.7 ± 0.8 to 3.1 ± 0.2 × 10^{-8} cm^2/s), suggesting an effect of the increased membrane crowding when reconstituting OppBCDF at protein/lipid ratios of 1:20 (w/w). Taken together the data indicate that liganded OppA binds specifically to OppBCDF, but the autocorrelation measurements alone are not sufficient to perform a detailed analysis of the OppA/OppBCDF interaction.

Fluorescence cross-correlation measurements

To monitor the binding of OppA to OppBCDF by FCCS, a single-cysteine mutant of the OppC component of OppBCDF was constructed. OppA (I602C) and OppBC(I296C)DF were purified, labeled with Alexa Fluor 488 or Alexa Fluor 633 (Fig. 1), respectively, and functionally incorporated into GUVs. As anticipated from previous results (19), all combinations of labeled SBPs and membrane complexes were active in peptide binding as well as transport (Table 2). Again, a relatively high concentration of OppA (1:50 (w/w) protein/lipid ratio) was used because of the anticipated low affinity interaction of the SBP with its membrane complex (13). The amount of coreconstituted OppBCDF was lowered to 1:100 (w/w), such that the final concentrations of the different proteins used in the FCCS experiments were equivalent to those used previously in uptake assays with proteo-LUVs and radioactive peptides (13). This experimental setup also more closely resembles the in vivo situation in which an excess of OppA over OppBCDF exists. The maximal fluorescence cross-correlation amplitude G_{cc}^{max} that can be obtained in this situation, assuming that Alexa Fluor 633-labeled OppBCDF binds Alexa Fluor 488-labeled OppA in a 1:1 stoichiometry, is given by:

$$G_{cc}^{max} = 2\,\frac{\omega_{488}^2}{\omega_{488}^2 + \omega_{633}^2}\,G_{488}, \qquad (1)$$

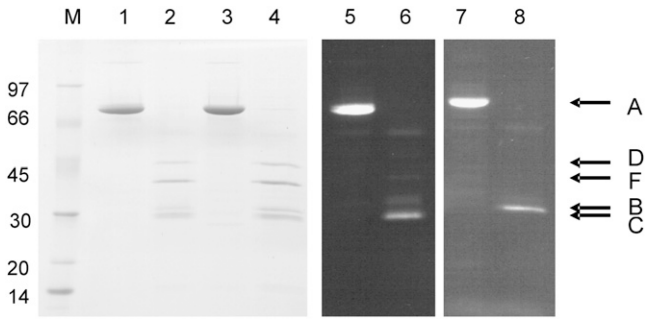

FIGURE 1 Purification and fluorescent labeling of single-cysteine Opp variants. Ni^{2+}- nitrilotriacetic acid purified OppA I602C was labeled with Alexa Fluor 488 (*lanes 1* and *5*) or 633 (*lanes 3* and *7*). OppBC(I296C)DF labeled with Alexa Fluor 488 (*lanes 2* and *6*), or 633 (*lanes 4* and *8*) is also shown. The proteins were visualized with either Coomassie brilliant blue staining (*lanes 1–4*), or by illumination using UV-light (*lanes 5–8*). The latter allowed verification of the attachment of the fluorophores to the proteins. The positions of the OppABCDF proteins are indicated as are the masses of the molecular mass marker (*M*) proteins (*kDa*).

where G_{488} is the amplitude of the green channel, and ω_{488} and ω_{633} are the lateral radii of the 488 and 633 confocal volumes, respectively. Note that this equation holds for a two-dimensional system and is only valid when an excess of Alexa Fluor 488-labeled OppA is present over Alexa Fluor 633-labeled OppBCDF. In the reverse situation, that is with 1:50 (w/w) Alexa Fluor 633-labeled OppA and 1:100 (w/w) Alexa Fluor 488-labeled OppBCDF, the amplitude of the autocorrelation curve from the 633 channel was nearly zero because of the high amount of OppA, and a cross-correlation signal could not be obtained (not shown).

OppBCDF distinguishes ligand-bound from ligand-free OppA

Fig. 2 *A* shows confocal scans of GUVs containing fluorescent-labeled OppA and OppBCDF. The observation volume was positioned on top of a GUV using a z-scan (Fig. 2 *B*). Fig. 2 *C* shows representative autocorrelation curves measured on GUVs containing Alexa Fluor 488-labeled OppA and Alexa Fluor 633-labeled OppBCDF. In the absence of peptide no cross-correlation signal was detected indicating that, on the timescale of the experiment, OppA was not associated with OppBCDF. On addition of 20 μM bradykinin (Fig. 2 *D*) the cross-correlation signal was 48 ± 15% with respect to the maximal possible signal (the latter corresponding to ~0.72 times the amplitude of the 488 channel as calculated using Eq. 1), suggesting that liganded OppA was bound to OppBCDF. A slight decrease in the mobility of OppBCDF was observed as well, which might have been because of OppA binding. However, the change in OppBCDF mobility was not statistically significant (from 2.3 ± 0.5 to 1.7 ± 0.6 × 10^{-8} cm^2/s). In conclusion, the cross-correlation measurements indicate that the membrane complex OppBCDF efficiently discriminates between OppA in its unliganded and liganded form and binds only the latter.

Oligomeric state of lipid-anchored OppA and OppA/OppBCDF binding stoichiometry

To investigate the oligomeric state of membrane-anchored OppA and the OppA/OppBCDF binding stoichiometry, Alexa Fluor 488- and Alexa Fluor 633-labeled OppAs were mixed 1:1 and coreconstituted into GUVs at a 1:100 (w/w) protein/lipid ratio (total OppA/lipid ratio of 1:50 (w/w)), in the absence or presence of nonlabeled OppBCDF. If, for example, OppA were a dimer, 488- and 633-labeled proteins would form 488-labeled homodimers, 488/633-labeled heterodimers, and 633-labeled homodimers, in a 1:2:1 ratio, respectively. The heterodimers should give rise to a cross-correlation signal. Assuming all OppAs would be present as dimers, G_{cc}^{max} is given by:

$$G_{cc}^{max} = \frac{2}{3}\,\frac{\omega_{633}^2}{\omega_{488}^2 + \omega_{633}^2}\,G_{633}, \qquad (2)$$

TABLE 2 Peptide binding and transport activity of fluorescent-labeled Opp reconstituted into LUVs

SBP*	Membrane complex†	Binding activity (nmol [^{3}H]-bradykinin/mg OppA)‡	Transport activity (pmol [^{3}H]-bradykinin/mg OppBCDF*min)§
OppA	–	14 ± 0¶	–‖
OppA-488**	–	14 ± 1¶	n.d.
OppA-633††	–	n.d.	n.d.
OppA	OppBCDF	n.d.	70 ± 34
OppA-488	OppBCDF	n.d.	74 ± 26
OppA-633	OppBCDF	n.d.	90 ± 25
OppA-488	OppBCDF-633‡‡	n.d.	60 ± 4
OppA-633	OppBCDF-488§§	n.d.	90 ± 8

n.d., not determined.
*OppA and labeled variants were reconstituted at a 1:50 (w/w) protein/lipid ratio.
†OppBCDF and labeled variants were reconstituted at a 1:100 (w/w) protein/lipid ratio.
‡The concentration of [^{3}H]-bradykinin was 3 μM.
§The concentration of [^{3}H]-bradykinin was 0.7 μM. Measurements were done in at least two independent experiments; mean ± SD values are given.
¶Taken from Doeven and colleagues (19).
‖Taken from Doeven and colleagues (13).
**OppA (I602C) labeled with Alexa Fluor 488.
††OppA (I602C) labeled with Alexa Fluor 633.
‡‡OppBC(I296C)DF labeled with Alexa Fluor 633.
§§OppBC(I296C)DF labeled with Alexa Fluor 488.

where G_{633} is the amplitude of the red channel, and ω_{488} and ω_{633} are again the respective radii of the 488 and 633 confocal volumes. Note that, as with Eq. 1, Eq. 2 describes the situation for a two-dimensional system. Thus, if OppA were dimeric, a cross-correlation signal would be observed with maximal amplitude of ~0.24 times that of the 633 curve.

Fig. 3 *A* and Table 3 show that no cross-correlation signal was obtained with proteo-GUVs containing ''double''-labeled OppA. Addition of 20 μM peptide had no effect on the fluorescence cross-correlation, which indicates that the oligomeric state of both the unliganded and liganded forms of membrane-bound OppA is monomeric. When OppBCDF was present in the proteo-GUVs as well, no cross-correlation signal was obtained both in the absence and presence of 20 μM bradykinin. Control experiments with double-labeled DNA (Fig. 3 *B*) confirmed that the cross-correlation efficiency of the setup was better than 80%, as described previously

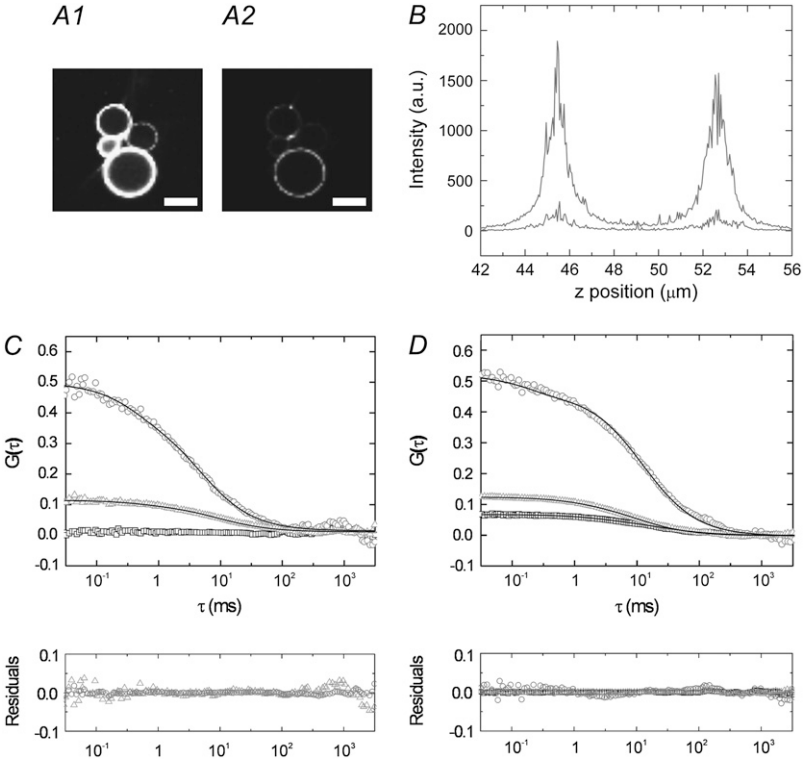

FIGURE 2 Confocal scans and FCCS measurements on fluorescent Opp-containing proteo-GUVs. (*A*) Two-dimensional cross sections obtained by (*x*,*y*) confocal imaging of proteo-GUVs containing Alexa Fluor 488-labeled OppA I602C (OppA-AF488) and Alexa Fluor 633-labeled OppBC(I296C)DF (OppBCDF-AF633). Images from the 488 (*A1*) and 633 (*A2*) channels are shown. The scale bars are 10 μm. (*B*) Typical z-scan used to localize the proteo-GUV membranes. Signals in the 488 and 633 channels are shown (*high* and *low intensity traces*, respectively). An excess of OppA-AF488 over OppBCDF-AF633 was incorporated in the GUVs (see text for details). (*C*) FCCS experiment in 20 mM K-Hepes, pH 8.0. The observation volumes were focused on top of a proteo-GUV. Autocorrelation signals from OppA-AF488 (Δ) and OppBCDF-AF633 (○) are shown. No cross-correlation signal (*lower curve,* □) was detected. (*D*) FCCS experiment in 20 mM K-Hepes, pH 8.0, plus 20 μM peptide (bradykinin). The presence of a cross-correlation signal (*lower curve,* □) indicates that OppA-AF488 and OppBCDF-AF633 were bound. Curves were fit with a one-component, two-dimensional diffusion model (*solid lines*), and the residuals are shown below the graph.

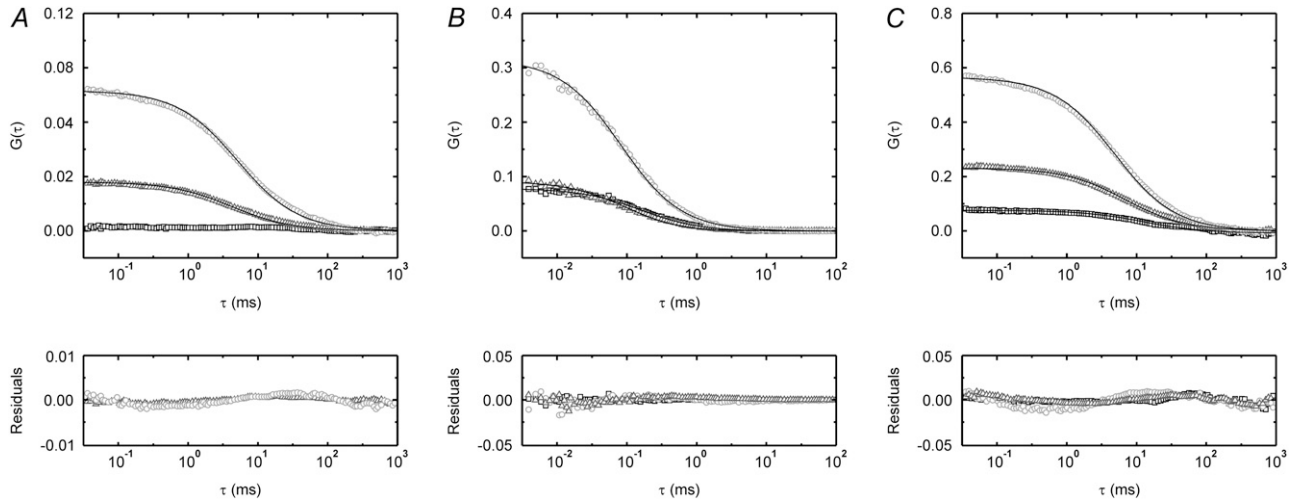

FIGURE 3 FCCS measurements on dual-labeled OppA and control samples. (*A*) Proteo- GUVs in which equimolar amounts of OppA-AF488 and OppA-AF633 were co-reconstituted (both at 1:100 (w/w) protein/lipid ratio). (*B*) AF488/AF633 double-labeled DNA control sample. (*C*) Proteo-GUV sample in which LacS-AF488 and LacS-AF633 were coreconstituted (both at 1:1000 (w/w) protein/lipid ratio). Autocorrelation signals from the 488 (Δ), 633 (○), and cross-correlation (□) channels are shown. Curves in *A* and *C* were fit with a one-component, two-dimensional diffusion model (*solid lines*), those in *B* were fit with a one-component, three-dimensional diffusion model. The residuals are shown in the lower panels.

(27). Next, we also established the ability to measure a cross-correlation signal for self-interacting particles embedded in the membrane. For this measurement, we used a well-studied dimeric membrane protein, LacS, and coreconstituted LacS-AF488 and LacS-AF633 in a 1:1 ratio; for the labeling with Alexa dyes, the LacS C320A/A635C double mutant was used (19). Again, significant cross-correlation signals were detected (Fig. 3 *C*), indicative of the presence of LacS-AF488/LacS-AF633 heterodimers. Taken collectively, the data of this and the previous paragraph suggest that a single OppA, in the liganded conformation, binds to OppBCDF.

ATP-binding Induces OppA release from OppBCDF

To obtain more detailed information on the catalytic cycle of the Opp system, FCCS experiments were performed under various conditions of energy supply. Whereas in the presence of 20 μM bradykinin liganded OppA bound to OppBCDF (Fig. 2 *D*), inclusion of 3 mM ATP with 1 mM EDTA in addition to 20 μM of peptide dissipated the cross-correlation signal completely. The signal was only slightly reduced in the presence of 0.1 mM of ATP plus EDTA (Table 4). In the absence of Mg^{2+}, ABC transporters bind ATP but do not hydrolyze the nucleotide (3,5,28). Addition of 3 mM of the nonhydrolyzable ATP-analog MgAMP-PNP resulted in the same effect. The cross-correlation signal was also diminished in the presence of MgATP plus ortho-vanadate, the vanadate-trapped transition state condition. However, cross-correlation was observed in the presence of 20 μM bradykinin and 3 mM of caged-ATP, indicating that the mere presence of a high concentration of adenine nucleotide was not sufficient for dissipation of the FCCS signal (not shown). Taken together, these results suggest that binding of ATP to the NBDs results in a conformational change that releases OppA from the translocator (OppBCDF) complex.

TABLE 3 FCCS results with GUVs containing double-labeled OppA

Protein composition of GUVs		Additions to rehydration buffer		
OppA-AF488*	OppA-AF633†	OppBCDF‡	20 μM bradykinin	Cross-correlation signal (%)§
+	+	−	−	<5
+	+	−	+	<5
+	+	+	−	<5
+	+	+	+	<5

*OppA (I602C) labeled with Alexa Fluor 488 was reconstituted at a 1:100 (w/w) protein/lipid ratio.
†OppA (I602C) labeled with Alexa Fluor 633 was reconstituted at a 1:100 (w/w) protein/lipid ratio.
‡OppBCDF was reconstituted at a 1:100 (w/w) protein/lipid ratio.
§Percentage of the maximal possible cross-correlation signal with the combination of fluorescent labels used (Eq. 2). Results of at least two independent experiments of five measurements each are shown. $G(0)$ values ranged from 0.015 to 0.1 for AF633 and from 0.05 to 0.3 for AF488 and were maximally ~0.002 for the cross-correlation signals.

TABLE 4 FCCS results with GUVs containing Alexa Fluor 488-labeled OppA and Alexa Fluor 633-labeled OppBCDF in 1:50 and 1:100 (w/w) protein/lipid ratios

Additions to rehydration buffer		
20 μM bradykinin	(Mg−) nucleotides ± EDTA or Vi	Cross-correlation signal (%)*
−	−	<5
+	−	48 ± 15†
+	0.1 mM ATP + 1 mM EDTA	32 ± 6†
+	3 mM ATP + 1 mM EDTA	<5
+	3 mM Mg-AMP-PNP	<5
+	3 mM Mg-ATP + 0.5 mM Vi	<5

*Percentage of the maximal possible cross-correlation signal with the combination of fluorescent labels used (Eq. 1). Averages and SD values of at least two independent experiments of five measurements each are given.
†These numbers reflect a significant cross-correlation signal; the differences between the numbers is not significant.

DISCUSSION

We have analyzed the mechanism of oligopeptide transport by the ABC uptake system Opp by FCS and FCCS measurements under conditions mimicking intermediate stages of the translocation cycle. Importantly, these experiments were carried out with the proteins in the membrane-embedded state and under conditions at which the transporters were fully functional. Previous studies on SBP/TMD interactions mostly involved the use of detergent-solubilized proteins or permeabilized proteoliposomes (5,6). The OppBCDF complex was not very stable in detergent solution as concluded from size exclusion and blue-native polyacrylamide gel electrophoresis experiments (M. K. Doeven and B. Poolman, unpublished results). Binding of MalE to $MalFGK_2$ has been studied in permeabilized proteo-LUVs (6). However, for Opp, this would involve the use of OppA lacking its N-terminal lipid-modification, a more artificial situation compared to membrane-anchored OppA. Proteo-GUVs proved to be a very good alternative for studying receptor-translocator interactions in the oligopeptide transporter in a defined, close-to-native model membrane system.

Using proteo-GUVs, we previously showed that lipid-anchored OppA diffuses with the same speed as lipids whereas integral membrane proteins, such as OppBCDF, have a two- to threefold lower lateral mobility (19,20). Therefore, we investigated the OppA/OppBCDF interaction by measuring changes in diffusion speed. Binding of fluorescent-labeled OppA to nonlabeled OppBCDF should result in a shift of the autocorrelation curve toward longer diffusion times. In OppBCDF-containing GUVs the mobility of OppA was indeed slower, and, on addition of peptide, mobility was reduced even further (Table 1). However, in the absence of peptide, no distinction could be made between specific binding of OppA to OppBCDF and a reduced lateral mobility because of the mere presence of membrane-embedded protein complex. Such hindered diffusion in a relatively crowded membrane environment is not unlikely, since it is known that the presence of integral membrane proteins negatively effects lipid lateral mobility at the lipid/protein ratios used in our experiments (29,30).

To circumvent this problem, we turned to dual-color FCCS, a technique first experimentally realized by Schwille and colleagues (31). Although this remains a technically demanding technique, which can easily give rise to artifacts (e.g., crosstalk between the detector channels), experiments with double-labeled fluorescent DNA indicated that in our setup we had a stable, high degree of overlap between the two laser focal volumes (Fig. 3 *B*; (27)). The overall FCCS efficiency was as high as ~80%. Furthermore, with the Alexa dye couple used in our experiments, the contribution of crosstalk to the cross-correlation signal was negligible (<5%). Single-cysteine mutants of OppA and OppBCDF, the latter bearing the cysteine substitution in one of the subunits of the integral membrane complex (OppC), were used for labeling with Alexa Fluor 488 or 633 maleimide (Fig. 1). In each case the position of the cysteine was chosen in the C-terminal part of the protein just in front of the His_6-tag used for purification, and, as expected, labeling had no effect on peptide binding or on transport activity ((19); Table 2). The fluorophore that is attached to OppA presumably sticks out from the surface of the protein (based on crystal structures of OppA homologs (32–35)), whereas the one that is attached to OppC is located in a short stretch of amino acids after the last helix that traverses the membrane back to the cytoplasmic side (36).

SBPs of ABC importers have been crystallized in open-unliganded, open-liganded, closed-liganded, and closed-unliganded conformations (34,37–39). In the presence of substrate, the equilibrium is thought to lie strongly toward the closed-liganded state, and only SBPs in this conformation would interact productively with the membrane components. Experiments with the histidine and maltose permeases, however, revealed that SBPs in their unliganded form(s) might also have access to the membrane complex, thereby impairing transport function (14–16). BtuF, the SBP of the vitamin B_{12} transporter, was shown to bind to detergent-solubilized BtuCD even in the absence of substrate (40), and this SBP may not dissociate from the membrane complex at all during the catalytic cycle (10,11). The dual-color FCCS experiments presented in Fig. 2 *C* and *D* revealed that OppBCDF distinguishes substrate-bound from substrate-free OppA, which is in line with previous results where inhibition of transport activity by high levels of unliganded SBP (as observed for the histidine and maltose transporters) could not be demonstrated for the Opp system (13). Next to the possibility that OppBCDF discriminates liganded from unliganded SBP, a second explanation would be that the equilibrium in the absence of substrate lies more strongly toward the open conformation for OppA compared with other SBPs such as HisJ, MalE, and BtuF, the SBPs of the afore mentioned histidine, maltose, and vitamin B_{12} transporters, respectively. This explanation would mean that the inhibition of transport

observed with the maltose and histidine transporters was caused by blocking of the membrane complex by SBPs in the closed-unliganded state. Of the various possibilities, we favor the scenario that OppBCDF discriminates liganded from unliganded SBP.

Although it is generally assumed that the oligomeric state of SBPs is monomeric, several early reports on these types of proteins suggest that they are dimeric (41–44). Moreover, ABC transporters have been found that have either one or two SBPs fused to the translocator, resulting in the presence of two or four SBPs per functional complex (45). Interaction between SBPs stimulated transport activity of the osmoregulatory ABC transporter OpuA from *L. lactis* (46). Fig. 3 *A* and Table 3 show that a cross-correlation signal was not detected in proteo-GUVs with Alexa Fluor 488 and 633-labeled OppA coreconstituted, which strongly suggests that lipid-anchored OppA does not form higher oligomeric aggregates. Addition of 20 μM peptide and/or inclusion of OppBCDF in the OppA-containing GUVs did not change the cross-correlation signals (not shown). Furthermore, sedimentation velocity and equilibrium centrifugation experiments also showed that OppA (without lipid anchor) is monomeric over a wide range of conditions tested (M. K. Doeven and B. Poolman, unpublished results). These results indicate that monomeric OppA binds peptide and that a single (liganded) OppA molecule binds to OppBCDF and is sufficient for transport.

In case of the maltose transporter (Fig. 4 *A*), it has been shown that on ATP binding to the substrate-loaded MalE: $MalFGK_2$ complex MalE opens (step III; (5)). At this stage maltose is thought to be donated to a site in the TMDs, MalF and G, or released into the cytoplasm directly. ATP hydrolysis is required to dissociate unliganded MalE from $MalFGK_2$ and to complete the transport cycle (step IV; (6)). Our results with the oligopeptide transporter (Fig. 4 *B*) show that ATP binding is sufficient to dissociate OppA from OppBCDF (step III). The ATP-dependent release of OppA was observed under conditions that preclude nucleotide hydrolysis (ATP without Mg^{2+} and excess of EDTA; use of the nonhydrolyzable analog AMP-PNP) and conditions that stabilize the transition state (Mg-ATP with *ortho*-vanadate). *Ortho*-vanadate has been previously shown to be an effective inhibitor of Opp-mediated transport (47) presumably by trapping the transition state (6,28). These observations suggest that on binding of ATP the peptide may have already been donated to a binding site in the membrane. ATP-hydrolysis and subsequent release of ADP and Pi would then reorient this site to complete the catalytic cycle (step IV). The fact that OppA dissociates as soon as ATP is bound whereas MalE merely opens but is not released (e.g., in the presence of *ortho*-vanadate) might be explained by the above discussed observations that OppBCDF distinguishes liganded from unliganded SBP more efficiently (13,15).

Although the proposed mechanisms of SBP-dependent uptake systems thus appear somewhat variable in respect to the timing of SBP/TMD interactions during the catalytic cycle, a comparison with the proposed mechanism for ABC

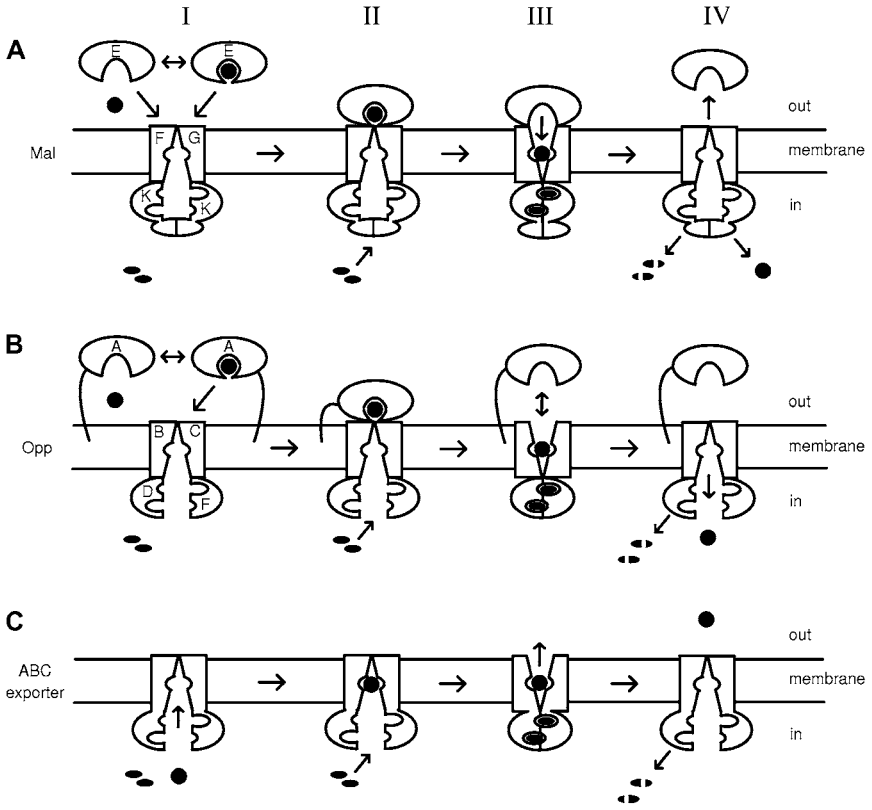

FIGURE 4 Mechanistic models for maltose (*Mal*) and oligopeptide (*Opp*) uptake and comparison to an ABC efflux system. Transport substrate and Mg-ATP are indicated by solid circles and ovals, respectively. Hydrolyzed ATP is depicted as split ovals. For simplicity, it is assumed that each system binds and hydrolyzes two molecules of ATP per translocation cycle. Further explanation is provided in the Discussion.

efflux systems (Fig. 4 *C*; (3,4)) reveals important conserved features (48). The largest difference is in the way substrate is bound (Fig. 4, steps I and II). ABC uptake systems require SBPs to signal the availability of substrate on the outside, whereas in ABC exporters the TMD binding site is readily accessible from the cytoplasmic face of the membrane. For both ABC importers and exporters, ATP-binding is thought to result in an altered accessibility of this TMD binding site in respect to the face of the membrane (step III; (3,4)). In ABC uptake systems this means that substrate now can enter the channel, whereas in the case of ABC export, substrate is released into the external medium. A second common feature is that on ATP-hydrolysis the transporter is thought to return to its initial conformation, thereby completing the catalytic cycle (step IV).

SUPPLEMENTARY MATERIAL

To view all of the supplemental files associated with this article, visit www.biophysj.org.

We thank Chris van der Does for valuable discussions and critical reading of the manuscript.

This work was supported by ''Top-subsidie'' grant 700-50-302 from the Netherlands Organization for Scientific Research-Chemische Wetenschappen (to B.P.) and funding from the Zernike Institute for Advanced Materials.

REFERENCES

1. Biemans-Oldehinkel, E., M. K. Doeven, and B. Poolman. 2006. ABC transporter architecture and regulatory roles of accessory domains. *FEBS Lett.* 580:1023–1035.
2. Higgins, C. F. 1992. ABC transporters: from microorganisms to man. *Annu. Rev. Cell Biol.* 8:67–113.
3. Higgins, C. F., and K. J. Linton. 2004. The ATP switch model for ABC transporters. *Nat. Struct. Mol. Biol.* 11:918–926.
4. Van der Does, C., and R. Tampé. 2004. How do ABC transporters drive transport? *Biol. Chem.* 385:927–933.
5. Austermuhle, M. I., J. A. Hall, C. S. Klug, and A. L. Davidson. 2004. Maltose-binding protein is open in the catalytic transition state for ATP hydrolysis during maltose transport. *J. Biol. Chem.* 279:28243–28250.
6. Chen, J., S. Sharma, F. A. Quiocho, and A. L. Davidson. 2001. Trapping the transition state of an ATP-binding cassette transporter: evidence for a concerted mechanism of maltose transport. *Proc. Natl. Acad. Sci. USA.* 98:1525–1530.
7. Chen, J., G. Lu, J. Lin, A. L. Davidson, and F. A. Quiocho. 2003. A tweezers-like motion of the ATP-binding cassette dimer in an ABC transport cycle. *Mol. Cell.* 12:651–661.
8. Ames, G. F.-L., C. E. Liu, A. K. Joshi, and K. Nikaido. 1996. Liganded and unliganded receptors interact with equal affinity with the membrane complex of periplasmic permeases, a subfamily of traffic ATPases. *J. Biol. Chem.* 271:14264–14270.
9. Liu, C. E., P. Q. Liu, A. Wolf, E. Lin, and G. F. Ames. 1999. Both lobes of the soluble receptor of the periplasmic histidine permease, an ABC transporter (traffic ATPase), interact with the membrane-bound complex. Effect of different ligands and consequences for the mechanism of action. *J. Biol. Chem.* 274:739–747.
10. Borths, E. L., B. Poolman, R. N. Hvorup, K. P. Locher, and D. C. Rees. 2005. In vitro functional characterization of BtuCD-F, the *Escherichia coli* ABC transporter for vitamin B_{12} uptake. *Biochemistry.* 44:16301–16309.
11. Hvorup, R. N., B. A. Goetz, M. Niederer, K. Hollenstein, E. Perozo, and K. P. Locher. 2007. Asymmetry in the structure of the ABC transporter binding protein complex BtuCD-BtuF. *Science.* 317:1387–1390.
12. Tynnkynen, S., G. Buist, E. Kunji, J. Kok, B. Poolman, G. Venema, and A. Haandrikman. 1993. Genetic and biochemical characterization of the oligopeptide transport system of *Lactococcus lactis*. *J. Bacteriol.* 175:7523–7532.
13. Doeven, M. K., R. Abele, R. Tampé, and B. Poolman. 2004. The binding specificity of OppA determines the selectivity of the oligopeptide ATP-binding cassette transporter. *J. Biol. Chem.* 279:32301–32307.
14. Dean, D. A., L. I. Hor, H. A. Shuman, and H. Nikaido. 1992. Interaction between maltose-binding protein and the membrane-associated maltose transporter complex in *Escherichia coli*. *Mol. Microbiol.* 6:2033–2040.
15. Merino, G., W. Boos, H. A. Shuman, and E. Bohl. 1995. The inhibition of maltose transport by the unliganded form of the maltose-binding protein of *Eschrichia coli*: experimental findings and mathematical treatment. *J. Theor. Biol.* 177:171–179.
16. Prossnitz, E., A. Gee, and G. F.-L. Ames. 1989. Reconstitution of the histidine periplasmic transport system in membrane vesicles. Energy coupling van interaction between the binding protein and the membrane complex. *J. Biol. Chem.* 264:5006–5014.
17. Schwille, P. 2001. Fluorescence correlation spectroscopy and its potential for intracellular applications. *Cell Biochem. Biophys.* 34:383–408.
18. Detmers, F. J., F. C. Lanfermeijer, R. Abele, R. W. Jack, R. Tampé, W. N. Konings, and B. Poolman. 2000. Combinatorial peptide libraries reveal the ligand-binding mechanism of the oligopeptide receptor OppA of *Lactococcus lactis*. *Proc. Natl. Acad. Sci. USA.* 97:12487–12492.
19. Doeven, M. K., J. H. Folgering, V. Krasnikov, E. R. Geertsma, G. van den Bogaart, and B. Poolman. 2005. Distribution, lateral mobility and function of membrane proteins incorporated into giant unilamellar vesicles. *Biophys. J.* 88:1134–1142.
20. Poolman, B., M. K. Doeven, E. R. Geertsma, E. Biemans-Oldehinkel, W. N. Konings, and D. C. Rees. 2005. Functional analysis of detergent-solubilized and membrane-reconstituted ABC transporters. *Methods Enzymol.* 400:429–459.
21. Rigaud, J. L., B. Pitard, and D. Levy. 1995. Reconstitution of membrane proteins into liposomes: application to energy-transducing membrane proteins. *Biochim. Biophys. Acta.* 1231:223–246.
22. Aragón, S. R., and R. Pecora. 1975. Fluorescence correlation spectroscopy as a probe of molecular dynamics. *J. Chem. Phys.* 64:1791–1803.
23. Elson, E. L., and D. Magde. 1974. Fluorescence correlation spectroscopy. I. Conceptual basis and theory. *Biopolymers.* 13:1–27.
24. Lowry, O. H., N. J. Rosebrough, A. L. Farr, and R. J. Randall. 1951. Protein measurement with the Folin phenol reagent. *J. Biol. Chem.* 165:265–275.
25. Saffman, P. G., and M. Delbrück. 1975. Brownian motion in biological membranes. *Proc. Natl. Acad. Sci. USA.* 72:3111–3113.
26. Lanfermeijer, F. C., A. Picon, W. N. Konings, and B. Poolman. 1999. Kinetics and consequences of binding of nona- and dodecapeptides to the oligopeptide-binding protein (OppA) from *Lactococcus lactis*. *Biochemistry.* 38:14440–14450.
27. Veldhuis, G., M. Hink, V. Krasnikov, G. van den Bogaart, J. Hoeboer, A. J. Visser, J. Broos, and B. Poolman. 2006. The oligomeric state and stability of the mannitol transporter, EnzymeII(mtl), from *Escherichia coli*: a fluorescence correlation spectroscopy study. *Protein Sci.* 15:1977–1986.
28. Davidson, A. L., and J. Chen. 2004. ATP-binding cassette transporters in bacteria. *Annu. Rev. Biochem.* 73:241–268.
29. O'Leary, T. J. 1987. Lateral diffusion of lipids in complex biological membranes. *Proc. Natl. Acad. Sci. USA.* 84:429–433.
30. Vaz, W. L. C., R. Goodsaid-Zalduondo, and K. Jacobson. 1984. Lateral diffusion of lipids and proteins in bilayer membranes. *FEBS Lett.* 174:199–207.

31. Schwille, P., F. Meyer-Almes, and R. Rigler. 1997. Dual-color fluorescence cross-correlation spectroscopy for multicomponent diffusional analysis in solution. *Biophys. J.* 72:1878–1886.

32. Dunten, P., and S. L. Mowbray. 1995. Crystal structure of the dipeptide binding protein from *Escherichia coli* involved in active transport and chemotaxis. *Protein Sci.* 4:2327–2334.

33. Levdikov, V. M., E. V. Blagova, J. A. Brannigan, L. Wright, A. A. Vagin, and A. J. Wilkinson. 2005. The structure of the oligopeptide-binding protein, AppA, from *Bacillus subtilis* in complex with a nonapeptide. *J. Mol. Biol.* 345:879–892.

34. Nickitenko, A. V., S. Trakhanov, and F. A. Quiocho. 1995. 2 Å resolution structure of DppA, a periplasmic dipeptide transport/chemosensory receptor. *Biochemistry.* 34:16585–16595.

35. Tame, J. R. H., G. N. Murshudov, E. J. Dodson, T. K. Neil, G. G. Dodson, C. F. Higgins, and A. J. Wilkinson. 1994. The structural basis of sequence-independent peptide binding by OppA protein. *Science.* 264:1578–1581.

36. Pearce, S. R., M. L. Mimmack, M. P. Gallagher, U. Gileadi, S. C. Hyde, and C. F. Higgins. 1992. Membrane topology of the integral membrane components, OppB and OppC, of the oligopeptide permease of *Salmonella typhimurium*. *Mol. Microbiol.* 6:47–57.

37. Heddle, J., D. J. Scott, S. Unzai, S-Y. Park, and J. R. H. Tame. 2003. Crystal structures of the liganded and unliganded nickel-binding protein NikA from *Escherichia coli*. *J. Biol. Chem.* 278:50322–50329.

38. Karpowich, N. K., H. H. Huang, P. C. Smith, and J. F. Hunt. 2003. Crystal structures of the BtuF periplasmic-binding protein for vitamin B12 suggest a functionally important reduction in protein mobility upon ligand binding. *J. Biol. Chem.* 278:8429–8434.

39. Trakhanov, S., N. K. Vyas, H. Luecke, D. M. Kristensen, J. Ma, and F. A. Quiocho. 2005. Ligand-free and -bound structures of the binding protein (LivJ) of the *Escherichia coli* ABC leucine/isoleucine/valine transport system: trajectory and dynamics of the interdomain rotaion and ligand specificity. *Biochemistry.* 44:6597–6608.

40. Borths, E. L., K. P. Locher, A. T. Lee, and D. C. Rees. 2002. The structure of *Escherichia coli* BtuF and binding to its cognate ATP binding cassette transporter. *Proc. Natl. Acad. Sci. USA.* 99:16642–16647.

41. Antonov, V. K., S. L. Alexandrov, and T. I. Vorotyntseva. 1976. Reversible association as a possible regulatory mechanism for controlling the activity of the non-specific leucine-binding protein from *Eschericha coli*. *Adv. Enzyme Regul.* 14:269–278.

42. Rashed, I., H. Shuman, and W. Boos. 1976. The dimer of the *Escherichia coli* galactose-binding protein. *Eur. J. Biochem.* 69:545–550.

43. Richarme, G. 1982. Associative properties of the *Escherichia coli* galactose binding protein and maltose binding protein. *Biochem. Biophys. Res. Commun.* 105:476–481.

44. Richarme, G. 1983. Associative properties of the *Escherichia coli* galactose-binding protein and maltose-binding protein. *Biochim. Biophys. Acta.* 748:99–108.

45. Van der Heide, T., and B. Poolman. 2002. ABC transporters: one, two or four extracytoplasmic substrate-binding sites? *EMBO Rep.* 3:938–943.

46. Biemans-Oldehinkel, E., and B. Poolman. 2003. On the role of the two extracytoplasmic substrate-binding domains in the ABC transporter OpuA. *EMBO J.* 22:5983–5993.

47. Kunji, E. R. S., E. J. Smid, R. Plapp, B. Poolman, and W. N. Konings. 1993. Di-tripeptides and oligopeptides are taken up via distinct transport mechanisms in *Lactococcus lactis*. *J. Bacteriol.* 175:2052–2059.

48. Dawson, R. J., K. Hollenstein, and K. P. Locher. 2007. Uptake or extrusion: crystal structures of full ABC transporters suggest a common mechanism. *Mol. Microbiol.* 65:250–257.